Development an Active-Caster with Differential Mechanism Utilizing a Twisted-Timing-Belt

Yuki Ueno[1 [0000−0003−2929−8595]], Issei Ikemura[1], and Haruhisa Ueda[1]

Tokyo University of Technology, 1404-1 Katakuramachi, Hachioji, 192-0982, Tokyo, Japan uenoyk@stf.teu.ac.jp
https://sites.google.com/edu.teu.ac.jp/humech-lab/english

Abstract. In this study, we developed an active-caster mechanism using a differential mechanism with a twisted-timing-belt and verified its operation with a prototype. The active caster enables omni-directional movement using standard tires, effectively addressing these concerns. However, conventional active casters drive the wheels and steering separately with different motors, resulting in inefficiencies in motor operation. To overcome this, we developed a mechanism that integrates the power of two motors using a differential mechanism with spur gears, distributing power to both the wheels and steering, and applied this technology to devices such as wheelchairs. Nevertheless, this approach faced reduced transmission efficiency due to the increased number of gear stages. Therefore, in this study, we propose a novel active caster mechanism employing a differential mechanism with a twisted-timing-belt. We elucidated the operational principles of this mechanism and derived a kinematic model. Furthermore, we constructed a prototype and validated its movement on a flat surface, confirming the feasibility of achieving omni-directional movement with our proposed mechanism.

Keywords: Omni-directional mobile mechanism · Active-caster · Differential mechanism.

1 Introduction

As the world grapples with declining birth rates and an aging population, there is an increasing demand for automation, labor-saving technologies, and efficiency improvements in workplaces. Omni-directional mobile robots, capable of moving in any direction, prove particularly effective in navigating tight spaces. However, conventional omni-directional mobile mechanisms typically employ free rollers on the outer circumference of wheels, which pose challenges such as limited rough terrain traversal capability, vibration, and low load capacity [1–3].

Research has explored driving these free rollers to enhance rough terrain traversal, yet issues with vibration and load capacity persist [4, 5]. In addition, there are instances where omni-directional movement has been achieved using crawler mechanisms to improve traversal capability. However, crawler mechanisms suffer from reduced efficiency on flat surfaces [6, 7].

Active casters represent another omni-directional mobile mechanism that enhances caster functionality through actuators [8]. By controlling the angular velocity of the wheel and the steering axis, active casters offer two degrees of freedom in translation. This capability allows equipment fitted with two or more active casters to move in all directions efficiently.

Conventional active casters utilize separate motors to drive the wheel and the steering axis. As a result, the motor for the steering axis operates only when the wheel is turning, remaining inactive during straight-line movement. This imbalance affects the motor operating efficiency. Additionally, when a wheel drive motor is mounted on the wheel axle, it rotates along with steering movements. Consequently, this setup presents a challenge in achieving infinite rotation due to wiring constraints imposed by the motor.

To address the limitation of the steering axis unable to rotate infinitely, Wada et al. developed a mechanism that utilizes ball transmission for power transfer [9]. In this mechanism, the power from two motors is transmitted to a ball, which in turn transmits it to another ball it contacts, thereby enabling rotation of both the wheels and steering axis.

The authors have developed an active caster mechanism that utilizes a differential mechanism to address both motor operation imbalances and the issue of the steering axis unable to rotate infinitely. The power from two motors is combined and distributed between the wheel and steering operations via the differential mechanism. This setup ensures that both motors are engaged simultaneously whether driving only the wheel or only the steering axis. Two types of mechanisms have been developed using planetary gears or spur gears [10, 11]. The spur gear type offers the advantage of requiring equal angular velocities and torques from both motors, allowing the use of motors with identical specifications.

As noted earlier, differential mechanisms are employed to combine the power of two motors and distribute it across two movements. For instance, the elbow joint of RIBA's arm features a differential mechanism utilizing bevel gears to extend the elbow and rotate the arm for pronation and supination [12]. Similarly, differential mechanisms using gears or linear motion systems are also employed in driving robot joints, offering benefits such as improved efficiency of mechanism drive and a more compact structure [13–15]. Furthermore, the rocker bogie mechanism used in planetary exploration rovers utilizes a differential mechanism with a linkage system to control the movement of the left and right arms independently [16].

Differential mechanisms employing gear or link mechanisms are susceptible to issues such as gear backlash and joint rattle in link mechanisms. Gear mechanisms, in particular, involve multiple gears, leading to problems such as noise, operational backlash, and reduced transmission efficiency affecting performance.

In this study, our aim is to propose a mechanism that implements a differential mechanism using a twisted-timing-belt and integrate it into an active caster. While mechanisms utilizing twisted-timing-belts for power transmission exist [17], there are no previous examples of employing it specifically for a differential

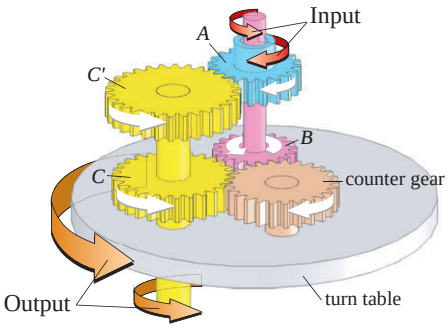

Fig. 1: Model of the differential mechanism utilizing spur gears [11]

mechanism. The use of a twisted-timing-belt in a differential mechanism is anticipated to yield a system with low noise, minimal backlash, and high transmission efficiency.

2 Active-Caster with Differential Mechanism by a Twisted-Timing Belt

2.1 Principle of the Conventional Mechanism

The authors have previously developed an active caster mechanism that utilizes a spur gear-type differential mechanism. A schematic diagram of the mechanism is shown in Fig. 1. Power from two motors is provided to gears A and B, respectively. The upper gear A meshes directly with gear C, while the lower gear B meshes with gear C' via a counter gear. Gears C and C' are fixed on the same axis, and the rotation of the wheel is achieved through a bevel gear and a timing belt. The rotation of the carrier, to which the gears are fixed, steers the wheel.

When gears A and B rotate in the same direction at the same speed, the same speed is transmitted to gears C and C' in the same direction. As a result, gears C and C' rotate in place, and this output is transmitted to the wheel.

Conversely, when gears A and B rotate in opposite directions at the same speed, the opposite rotations cancel each other out in gears C and C', causing them not to rotate. However, since gears A and B, which are on the same axis as the mechanism's center of rotation, are rotating in the same direction, the entire mechanism rotates. This rotation is then converted into steering motion.

2.2 Principle of the Proposed Mechanism

Figure 2 shows a schematic diagram of the differential mechanism utilizing a twisted timing belt, which achieves the same operation as a spur gear type mechanism. Input from two motors is transmitted to pulleys A and B at the

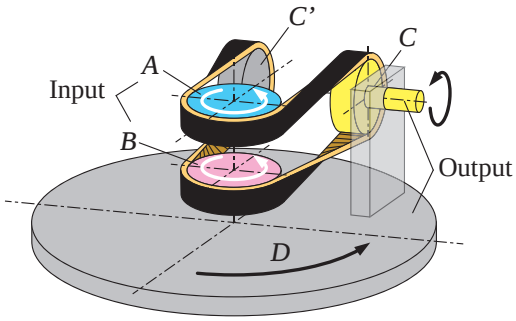

Fig. 2: Model of the differential mechanism utilizing a twisted timing belt

center of the mechanism. Pulleys C and C' are positioned on an axis perpendicular to the input pulleys, and power is transmitted by twisting the timing belt 90 degrees. Pulley C' rotates freely in place, while the power from pulley C is transmitted to the wheel via another timing belt.

When pulleys A and B rotate in opposite directions at the same speed, the timing belt transmits power from one pulley to the other, enabling them to rotate. This rotation powers the wheels.

Conversely, when pulleys A and B rotate in the same direction at the same speed, the belt does not move. However, similar to the conventional mechanism, since pulleys A and B, located at the center of the mechanism, are rotating in the same direction, the entire mechanism rotates, and this rotation becomes steering motion.

In the conventional mechanism, power is transmitted using five spur gears, bevel gears, and a timing belt. In contrast, the proposed mechanism transmits power using only two timing belts, thereby reducing the number of parts.

2.3 Kinematics

Omni-directional movement is achieved by controlling the angular velocities of the wheel and the steering axis. Consequently, the two motors are velocity-controlled.

The numbers of teeth of pulleys A, B, C, and C' are Z_A, Z_B, Z_C, and $Z_{C'}$, respectively. The input of this mechanism is the angular velocity from the motors, which is transmitted to pulleys A and B. The output is the angular velocity of pulley C and the carrier D, which is the angular velocity of the wheel and the steering axis.

Let the input vector be $u_d = [\omega_A, \omega_B]^\top$ and the output vector be $\boldsymbol{\omega_d} = [\omega_C, \omega_D]^\top$. The relationship between input and output is expressed as follows:

$$\boldsymbol{\omega_d} = \boldsymbol{B_d u_d}, \tag{1}$$

where,

$$\boldsymbol{B_d} = \begin{bmatrix} -\dfrac{\boldsymbol{Z_A}}{\boldsymbol{2Z_C}} & \dfrac{\boldsymbol{Z_B}}{\boldsymbol{2Z_C}} \\ \dfrac{\boldsymbol{1}}{\boldsymbol{2}} & \dfrac{\boldsymbol{1}}{\boldsymbol{2}} \end{bmatrix}. \tag{2}$$

The inverse kinematics model is as follows:

$$\boldsymbol{u_d} = \boldsymbol{B^{-1}\omega_d}, \tag{3}$$

where,

$$\boldsymbol{B_d^{-1}} = \begin{bmatrix} -\dfrac{\boldsymbol{2Z_C}}{\boldsymbol{Z_A + Z_B}} & \dfrac{\boldsymbol{2Z_B}}{\boldsymbol{Z_A + Z_B}} \\ \dfrac{\boldsymbol{2Z_C}}{\boldsymbol{Z_A + Z_B}} & \dfrac{\boldsymbol{2Z_A}}{\boldsymbol{Z_A + Z_B}} \end{bmatrix}. \tag{4}$$

ω_C and ω_D are transmitted to the wheel axis and steering axis, respectively. However, since the wheels rotate together with the steering axis, if we denote the angular velocities of the wheels and steering as ω_w and ω_s, respectively, then $\omega_w = \omega_C - \omega_D$ and $\omega_s = \omega_D$. The relationship between these angular velocities of the active caster, $\boldsymbol{u_w} = [\omega_w, \omega_s]^\top$, and the two translational degrees of freedom velocity of the active caster $\boldsymbol{x_w} = [x_w, y_w]^\top$, is as follows, as in reference [8, 10, 11].

$$\boldsymbol{\dot{x}_w} = \boldsymbol{B_w u_w}, \tag{5}$$

where,

$$\boldsymbol{B_w} = \begin{bmatrix} \boldsymbol{r_w}\cos\boldsymbol{\theta_w} & -\boldsymbol{l}\sin\boldsymbol{\theta_w} \\ \boldsymbol{r_w}\sin\boldsymbol{\theta_w} & \boldsymbol{l}\cos\boldsymbol{\theta_w} \end{bmatrix}. \tag{6}$$

The inverse kinematics model is as follows:

$$\boldsymbol{u_w} = \boldsymbol{B_w^{-1}\dot{x}_w}, \tag{7}$$

where,

$$\boldsymbol{B_w^{-1}} = \begin{bmatrix} \dfrac{\boldsymbol{1}}{\boldsymbol{r}}\cos\boldsymbol{\theta_w} & \dfrac{\boldsymbol{1}}{\boldsymbol{r}}\sin\boldsymbol{\theta_w} \\ -\dfrac{\boldsymbol{1}}{\boldsymbol{l}}\sin\boldsymbol{\theta_w} & \dfrac{\boldsymbol{1}}{\boldsymbol{l}}\cos\boldsymbol{\theta_w} \end{bmatrix}. \tag{8}$$

θ_w, r and l are the angle of the steering axis, the wheel radius, and the offset between the steering axis and the grounding point of wheel, respectively.

3 Experimental Machine

In this study, we develop an experimental machine that can be installed on an electric wheelchair. The specifications of the assumed wheelchair are shown in Table 1.

A 3D-CAD model of the designed mechanism is shown in Fig. 3. Pneumatic tires with a wheel diameter of 200 mm are used. A layout of the timing pulley in

Table 1: Specifications of assumed wheelchair

Size(D×W×H)	800×700×500 mm
Weight	70 kg
Loading capacity	80 kg
Motor power	200 W × 4
Max. velocity	1.67 m/s
Max. acceleration	2.0 m/s^2
Slope climbing capacity	10 deg
Max. step difference	40 mm

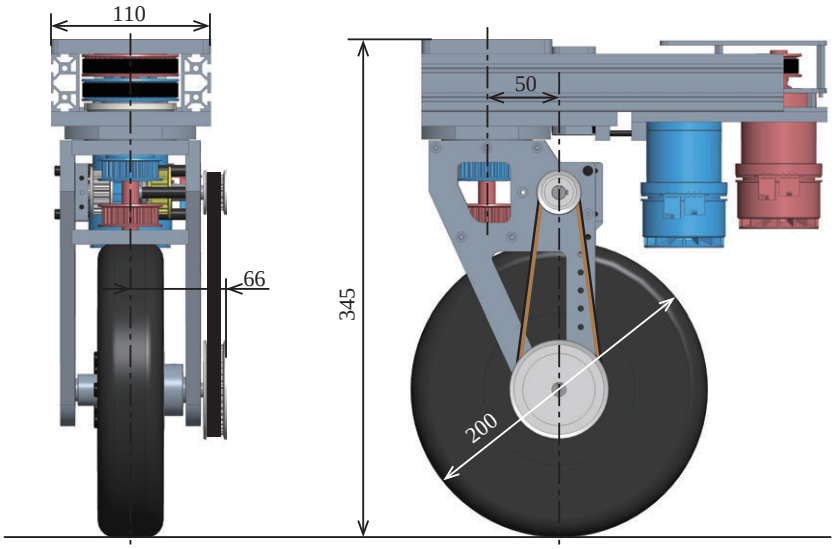

Fig. 3: 3D-CAD model of experimental active-caster

the differential mechanism shown in Fig. 4. The pitch circles of pulleys A and B and the pitch circles of pulleys C and C' overlap, with the pitch circles at their centers. This configuration allows the belt to mesh with the pulley teeth to the maximum extent, minimizing belt twist.

A cross-sectional view of the designed mechanism is shown in Fig. 5. Two brushless 200W motors with 4.3:1 reduction gears (Maxon Motor AG, EC flat ϕ60mm) are used, similar to the spur gear type DDSS developed in the authors' previous research [18]. The motors are controlled by servo controller ESCON 70/10 from Maxon Motor AG. An absolute encoder is used to measure the steering angle. As shown in the figure, pulleys A and B are arranged coaxially, with pulley B's axis passing through the inside of pulley A. This arrangement

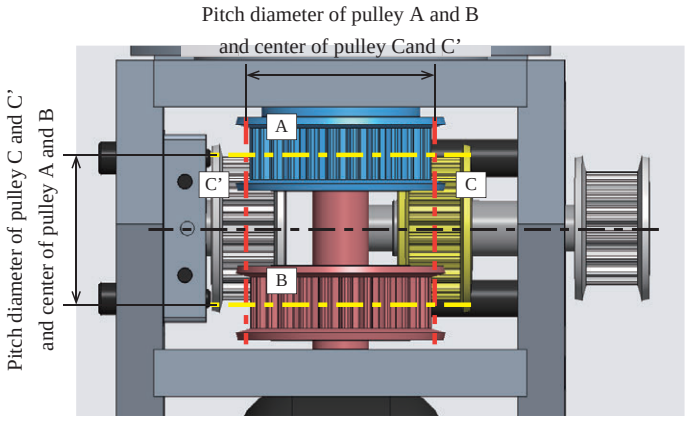

Fig. 4: Layout of timing pulleys

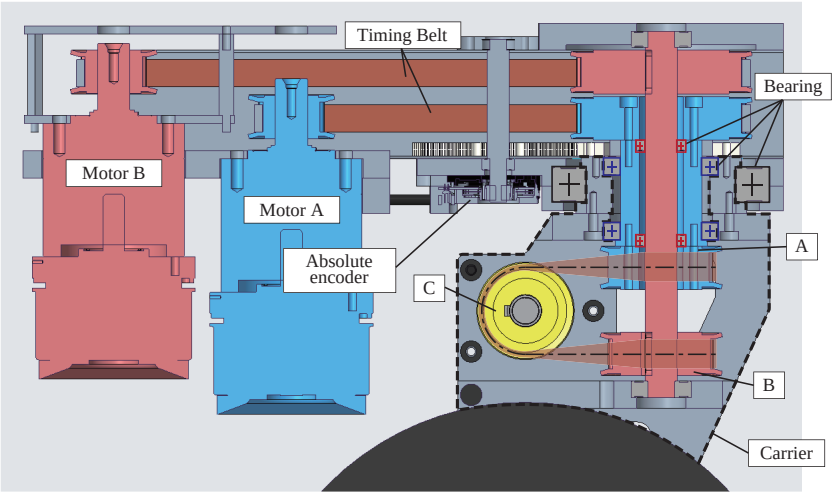

Fig. 5: Cross section of experimental active-caster

allows the pulleys to be placed compactly, transmitting power from two motors at the top of the mechanism.

4 Operation Verification Experiment

4.1 Experimental Conditions

To verify the movement capabilities of the proposed mechanism, we developed a device capable of moving freely on a flat surface using three linear guides (C-SXR42-1000), as shown in Fig. 6. A compression spring is placed between the

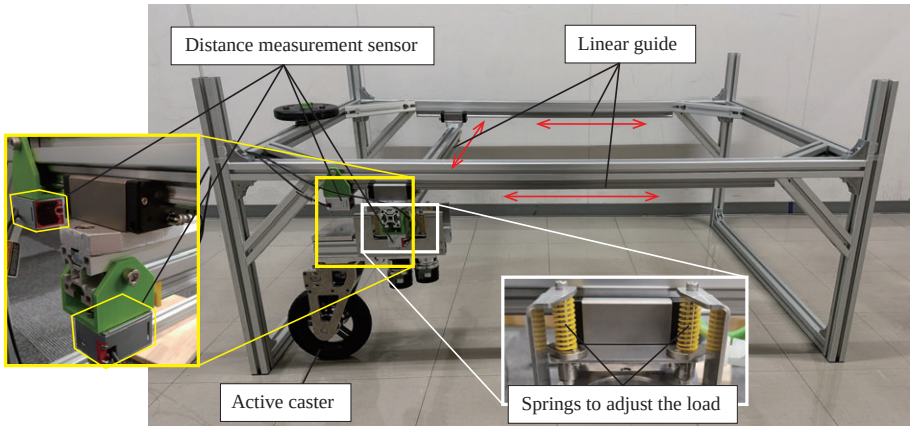

Fig. 6: Configurations of experimental system

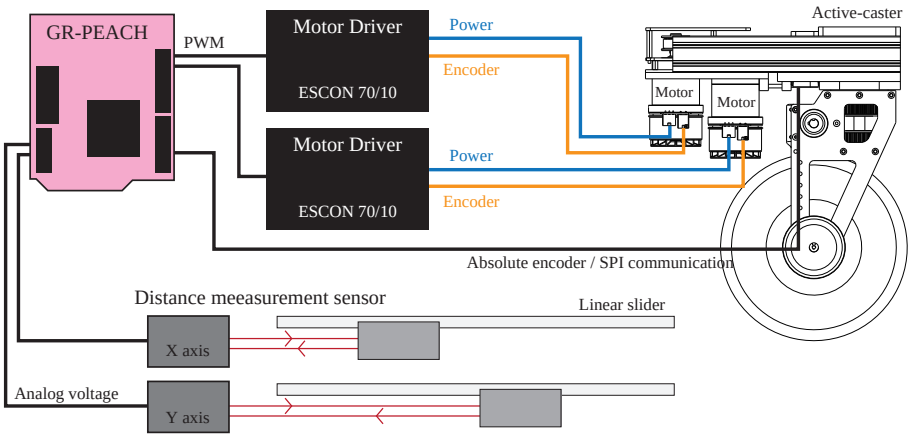

Fig. 7: Configurations of experimental system

mechanism and the frame to adjust the load by varying the degree of deformation. The mechanism is driven by motors, generating the driving force, while a distance measurement sensor (LR-TB5000, Keyence), which utilizes an infrared laser, is used to measure the travel distance.

The configuration of the experimental setup is shown in Fig. 7. Processing is performed using a single-board computer, GR-PEACH. The steering angle is obtained from an absolute encoder (AMT222, Digi International) via SPI communication.

Once the translational reference velocity of the mechanism is applied, the angular velocities of the wheel and the steering axis are calculated using Eq. (7). Additionally, the reference angular velocities of the two motors are calculated using Eq. (3). The command angular velocity for each motor is sent to the motor

driver using a PWM signal and a rotation direction signal. The motor driver then performs feedback control of the angular velocity based on these command signals.

The position of the slider is determined by converting the analog voltage output from distance measurement sensors via AD conversion. The sensor outputs a voltage range of 0 to 10 V corresponding to a measurement range of 0 to 1000 mm. To accommodate the microcontroller's input range of up to 3.3 V, the sensor's analog voltage is divided using resistors (10.2 kΩ and 4.99 kΩ). The microcontroller converts the scaled voltage range of 0 to 5 V into a digital value with a 10-bit resolution, resulting in a distance resolution of approximately 1.48 mm.

In the experiment, the initial state sets the wheels aligned along the X-axis. The active-caster mechanism travels a distance of 400 mm at a maximum speed of 0.1 m/s, changing its travel direction in 15-degree increments around the X-axis. The command velocity follows a trapezoidal pattern with a pre-generated acceleration of 0.1 m/s^2. As such, no feedback control is applied to the travel direction. The loads on the wheels consist of 1.2 kg, approximately equal to the mass of the active-caster mechanism itself, and an additional 8.4 kg from the compressed spring.

4.2 Experimental Results

The experimental results for the load of 1.2 kg are shown in Fig. 8, and the results for the load of 8.4 kg are shown in Fig. 9.

From the results, it can be seen that the active-caster mechanism travels along the target path when the direction of travel is 0 degrees. However, as the direction of travel angle increases, deviations in the trajectory become noticeable.

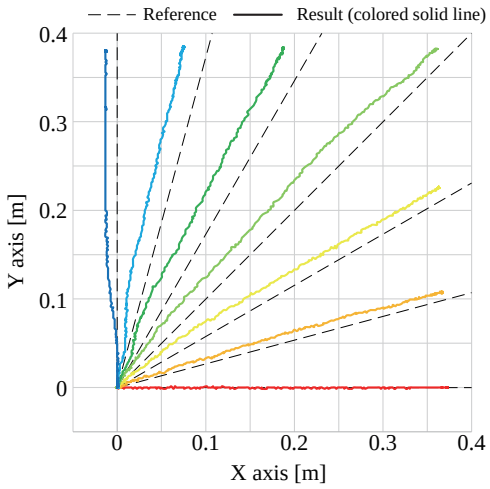

Fig. 8: Experimental result with a load of 1.2 kg

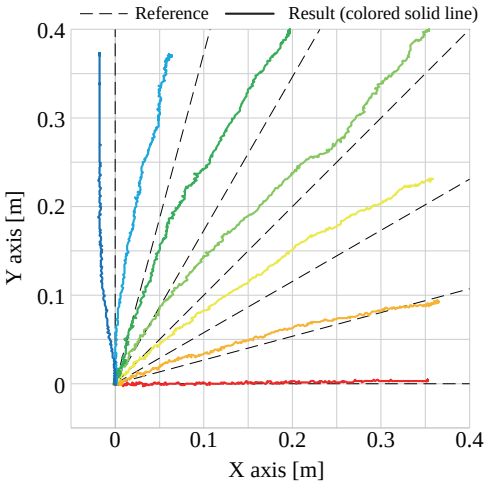

Fig. 9: Experimental result with a load of 8.4 kg

Table 2: Maximum deviation from target trajectory

	Maximum deviation [mm]						
Angle[deg]	0	15	30	45	60	75	90
1.2 kg	1.48	11.8	16.8	27.2	30.2	29.1	13.3
8.4 kg	4.44	10.7	34.6	34.6	41.8	39.9	19.3

The maximum deviation distance from the target trajectory is shown in Table 2. Since there are no significant changes after the initial deviation, it is likely caused by wheel friction during the initial steering.

Figure 10 shows the results of the reference angular velocity and the calculated angular velocity of the steering axis obtained using backward difference with the measured steering angle. The results confirm that there is a difference in angular velocity of the steering angle at the beginning of the movement.

However, since the active-caster mechanism can typically move in the commanded direction and path deviations can be mitigated through feedback control, it can be concluded that the proposed mechanism operates generally without issues.

5 Conclusion

In this study, we proposed an active caster mechanism with a differential mechanism using a twisted timing belt. While there are examples of using twisted timing belts for power transmission, there have been no examples of their use as a differential mechanism, making this a novel mechanism. Compared to conven-

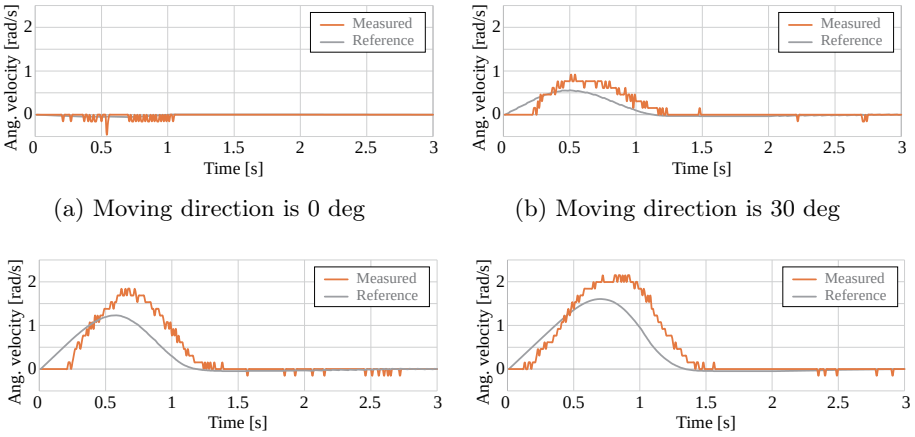

(a) Moving direction is 0 deg

(b) Moving direction is 30 deg

(c) Moving direction is 60 deg

(d) Moving direction is 90 deg

Fig. 10: Experimental result of angular velocity of steering axis

tional gear-based mechanisms, this mechanism is expected to reduce the number of parts, resulting in weight reduction, improved mechanical efficiency due to fewer gear stages, and noise reduction. In this paper, we first derived the kinematic model of the proposed mechanism. Next, we designed an experimental machine with specifications assuming wheelchair use. Furthermore, we developed an experimental device capable of two-degree-of-freedom planar travel using the experimental machine and conducted verification experiments. From the experimental results, although deviations in trajectory occurred due to discrepancies in steering angular velocity at the initial stage of operation, it was found that the mechanism could generally travel in the desired direction. This demonstrates that it is possible to control two translational degrees of freedom using the proposed mechanism and kinematic model.

Future challenges include measuring mechanical efficiency, evaluating noise, and verifying the operation of mobile robots using this mechanism.

References

1. Grabowiecki, J.: Vehicle-wheel, US Patent No. 1305535 (1919).
2. Ilon, B.E.: Directionally Stable Self Propelled Vehicle, US Patent No. 3746112 (1973).
3. Tadakuma, K., Tadakuma, R. and Berengeres, J.: Development of Holonomic Omnidirectional Vehicle with “Omni-Ball”: Spherical Wheels, Proceedings of International Conference on Intelligent Robots and Systems (IROS), pp. 33-39 (2007).
4. Komori, M., Matsuda, K., Terakawa, T., Takeoka, F., Nishihara, H., Ohashi, H.: Active omni wheel capable of active motion in arbitrary direction and omnidirectional vehicle, Journal of Advanced Mechanical Design, Systems, and Manufacturing, vol. 10, no. 6 pp. JAMDSM0086 (2016).

5. Ichimura, T., Tadakuma, K., Takane, E., Konyo, M. and Tadokoro, S.: Development of a spherical tether-handling device with a coupled differential mechanism for tethered teleoperated robots, Proceedings of International Conference on Intelligent Robots and Systems (IROS), pp. 2604-2609 (2016).
6. Tadakuma, K., Tadakuma, R., Nagatani, K., Yoshida, K., Peters, S., Udengaard, M. and Iagnemma, K.: Crawler vehicle with circular cross-section unit to realize sideways motion, Proceedings of International Conference on Intelligent Robots and Systems, pp. 2422-2428 (2008).
7. Takane, E., Tadakuma, K., Watanabe, M., Konyo, M. and Tadokoro, S.: Design and Control Method of a Planar Omnidirectional Crawler Mechanism, Journal of Mechanical Design, vol. 144, no. 1, pp. 013302 (2021).
8. Wada, M. and Mori, S.: Holonomic and omnidirectional vehicle with conventional tires, Proceedings of International Conference on Robotics and Automation (ICRA), pp. 3671-3676 (1996).
9. Wada, M., Inoue, Y. and Hirama, T.: A new active-caster drive system with a dual-ball transmission for omnidirectional mobile robots, Proceedings of International Conference on Intelligent Robots and Systems (IROS), pp. 2525-2532 (2012).
10. Ueno, Y., Ohno, T., Terashima, K. and Kitagawa, H.: The development of driving system with Differential Drive Steering System for omni-directional mobile robot, Proceedings of International Conference on Mechatronics and Automation, pp. 1089-1094 (2009).
11. Ueno, Y., Ohno, T., Terashima, K., Kitagawa, H., Funato, K. and Kakihara, K.: Novel differential drive steering system with energy saving and normal tire using spur gear for an omni-directional mobile robot, Proceedings of International Conference on Robotics and Automation (ICRA), pp. 3763-3768 (2010).
12. Mukai, T., Hirano, S., Nakashima, H., Kato, Y., Sakaida, Y., Guo, S. and Hosoe, S.: Development of a nursing-care assistant robot RIBA that can lift a human in its arms, Proceedings of International Conference on Intelligent Robots and Systems (IROS), pp. 5996-6001 (2010).
13. Park, M. -H. and Cho, B. -K.: Design of New Drive Mechanism for Dynamic Movement of Humanoid Robot Legs, Proceedings of International Conference on Humanoid Robots (Humanoids), pp. 1-8 (2023)
14. Cheon, S., Choi, W., Oh, S. -R. and Oh, Y.: Development of an underactuated robotic hand using differential gear mechanism, Proceedings of International Conference on Ubiquitous Robots and Ambient Intelligence (URAI), pp. 328-334 (2014).
15. Olaru, I. M. C., Krut, S. and Pierrot, F.: Novel mechanical design of biped robot SHERPA using 2 DOF cable differential modular joints, Proceedings of International Conference on Intelligent Robots and Systems (IROS), pp. 4463-4468 (2009).
16. Lindemann, R. A. and Voorhees, C. J.: Mars Exploration Rover mobility assembly design, test and performance, Proceedings of International Conference on Systems, Man and Cybernetics, vol. 1, pp. 450-455 (2005).
17. Perneder, R. and Osborne, I: Handbook Timing Belts, Springer Berlin, Heidelberg (2012).
18. Ueno, Y., Ikemura, I., Tanaka, T. and Matsuo, Y.: Development of a Front-Wheel-Steering-Drive Dual-Wheel Caster Drive Mechanism for Omni-Directional Wheelchairs with High Step Climbing Performance, Journal of Robotics and Mechatronics, vol. 34, no. 6, pp. 1431-1440 (2022).